The microstructural origin of rapid densification in 3YSZ during ultra-fast firing with or without an electric field

Wei Ji [1, 2], Jinyong Zhang [1], Weimin Wang [1], Zhengyi Fu [1], Richard Todd [2]*

1. State Key Laboratory of Advanced Technology for Materials Synthesis and Processing, Wuhan University of Technology, Wuhan 430070, China

2. University of Oxford, Department of Materials, Parks Road, Oxford OX1 3PH, UK

*Corresponding author: richard.todd@materials.ox.ac.uk;

Abstract:

Recent research has shown that very rapid heating of 3YSZ powder compacts (ultra-fast firing), whether by passing an electric current through the sample (flash sintering) or by using external heat sources, causes a great acceleration of densification rate for a given relative density and temperature. Here, the microstructural evolution of 3YSZ is studied using four sintering methods with widely differing heating rates, produced with and without electric fields. The microstructural development depended greatly on thermal history. Most significantly, slow, conventional heating resulted in pores much larger than the grain size, whereas most pores were smaller than the grain size with the rapid heating methods, whether the heating involved an electric field or not. The smaller pore size clearly provides a major contribution to the acceleration of densification following rapid heating. In contrast, grain growth was not suppressed by rapid heating but was suppressed by an electric field.

Key words: Flash sintering; grain growth; pore size; densification; YSZ

Introduction

Flash sintering is a technique whereby dense ceramics can be produced in a few seconds by passing an electric current through the specimen. The furnace temperature used is usually several hundred degrees centigrade below those used in conventional sintering, which normally takes several hours. The resulting reduction in time and energy consumed make it a potentially efficient way to fabricate advanced ceramics. The sintering method has been investigated extensively in

3YSZ and a wide range of other ceramics [1-7].

The electrical and thermal response of the specimen during flash sintering is explained well in terms of heating from the electrical power dissipation in the specimen [3,8,9]. Under constant electric field, this increases rapidly once a sufficiently high combination of temperature and field is reached owing to the strongly increasing electrical conductivity of most ceramics with increasing temperature, with increasing densification [10] and, in the case of YSZ, with electrochemical reduction resulting from the high direct currents passed through the specimen [10, 11]. Although the furnace temperature is low, the temperature of the specimen itself during flash sintering is typically raised by the electrical heating to close to the temperature used for the same material in conventional sintering.

The above explanation for the electrical and thermal response has been tested by many researchers with good, quantitative verification (e.g. [4,12,13]) but does not, on its own, provide any explanation for the rapid densification in flash sintering. Much of the search for an explanation has focused on the presence of an electric field, which is perhaps the most obvious difference between flash sintering and conventional sintering, but so far without convincing success. Another significant difference between conventional sintering and flash sintering, however, is the very rapid specimen heating during flash sintering, which is made possible by the internal dissipation of electrical power within the specimen. It has been known since the 1960's that rapid heating, or "fast firing", improves the extent and rate of densification. We have recently tested this idea as an explanation for flash sintering by comparing the densification of identical green bodies of 3YSZ by flash sintering and by rapid heating to the same specimen temperature, but without the use of electric fields [14]. The results show that heating at similar rates to those experienced by specimens during flash sintering can lead to the same rapid densification rates even without the involvement of an electric field. The inescapable implication is that the rapid densification during the flash sintering of 3YSZ occurs primarily because of the rapid heating experienced rather than any direct effect of the electric field itself.

Previous explanations for fast firing have mainly been based on the idea that densification competes with coarsening mechanisms such as grain growth [15] or surface diffusion [16,17,18] which oppose it. The coarsening mechanisms are thought to have different temperature dependencies to that of densification, so that the degree of densification and other aspects of

microstructural development have a dependence on the details of the thermal history such as prior heating rate. This is fundamentally different from the unique path of microstructural development which would result from the operation of a single densification mechanism. Our previous work [14] reports only the densification results for 3YSZ heated at different rates with and without an electric field. The present paper seeks possible explanations for the effect of heating rate by looking for differences in the path of microstructural development in specimens with different heating rates and heating sources. The comparison involves the same four sintering methods as were used in [14]: (i) flash sintering (FS), (ii) conventional sintering (CS), (iii) "fast firing" (FF) by inserting specimens into a ready heated furnace, and (iv) "ultra-fast firing" (SHS), in which very rapid heating is achieved without an electric field using an exothermic self-propagating reaction between Ni and Al powders as the heat source.

Experimental details

Raw material and green body:

All the raw materials in the experiments of this work were commercially available 3YSZ (TZ-3Y-E, Tosoh Co., Japan). As reported by the supplier, the median particle size of the starting powder is 60 nm and the density when conventionally sintered under optimum conditions is 6.05 g/cm^3.

The specimens for flash sintering (FS) were bar shaped with dimensions ~26 × 6 × 2 mm as described in [14]. These were made by the slip casting of slurries consisting of 55 wt.% 3YSZ powder and 2 wt. % Dispex A40 dispersant in distilled water into plastic moulds on a porous gypsum base. An ultrasonic probe was used to break up any agglomerates in the slurry. Metallic pins of 1 mm in diameter were set in the specimen 22 mm apart, near the ends of the bar, and removed before samples were completely dried, to leave holes for making the electric connections. Two short platinum wires with an initial separation of L = 14mm were set between the holes for 4-point electrical measurements to eliminate the effect of contact resistance. Final drying was in an oven at 80 °C. The resulting green bodies were approximately 55% dense.

The specimens for the other sintering methods (CS, FF and SHS) were small pieces with dimensions ~1-2mm separated from green samples identical to those used for FS. The small dimensions were to allow rapid heating from external heat sources throughout the specimen. The

sintering conditions for all the experiments are shown in Table 1.

Flash Sintering:

For flash sintering, experiments in which electric fields were applied to ceramic specimens through a closed electrical circuit were carried out in a modified box furnace. A schematic diagram of the flash sintering samples and apparatus is shown in Fig.1.

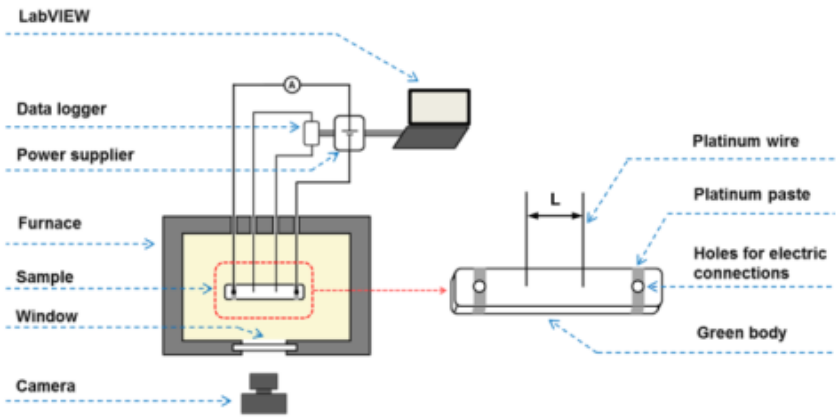

Figure 1. Schematic diagram of the flash sintering experiment.

A commercial DC power source (360 V, 15 A, 1500 W, Elektro-Automatik, Viersen, Germany) was used and the data were logged using LabView software. Green bodies were first pre-sintered in a tube furnace at 750 °C for an hour to develop sufficient strength for suspending from the wires. Platinum paste was applied on each electrode area of the pre-sintered body to promote electrical connection and current uniformity through the specimen during sintering. The suspended samples in the flash sintering furnace were then heated in the furnace at a rate of 7.5 °C/ min to 600 °C and then 5 °C / min to 925 °C. Electric fields of 150 V/cm were applied in all the flash sintering runs. The power supply was programmed to apply a constant voltage but was subject to a maximum current of 0.5 A. The sintering process was recorded by a video camera with a constant photo-sensitivity. The temperature of the specimen during flash sintering was estimated from the logged data by the using the non-equilibrium black body model first proposed in our previous work [14]:

$$T_s = T_f + \int_0^t \frac{VI - A\sigma\varepsilon\left(T_s^4 - T_f^4\right)}{mc_p}\,\mathrm{d}t \qquad (1)$$

Here V is voltage, I is current, A is the instantaneous surface area of the specimen, σ is Stefan's constant, ε is the emissivity, taken as 0.9 in this work, T_s and T_f are the temperatures of the specimen and the furnace respectively, m is the mass and c_p = 600 J kg^{-1} K^{-1} is the heat capacity of 3YSZ. The temperature during a typical flash sintering process is shown in Fig. 2. The temperature increased very rapidly from the furnace temperature to the peak value of 1347 ^oC following the application of the electrical field. This peak corresponds to the switch from voltage control to current control at which the electrical power dissipation is also a maximum. The temperature decreased to a steady value of 1280 ^oC over several seconds after the peak temperature point. The sample temperature dropped to the furnace temperature quickly after power off.

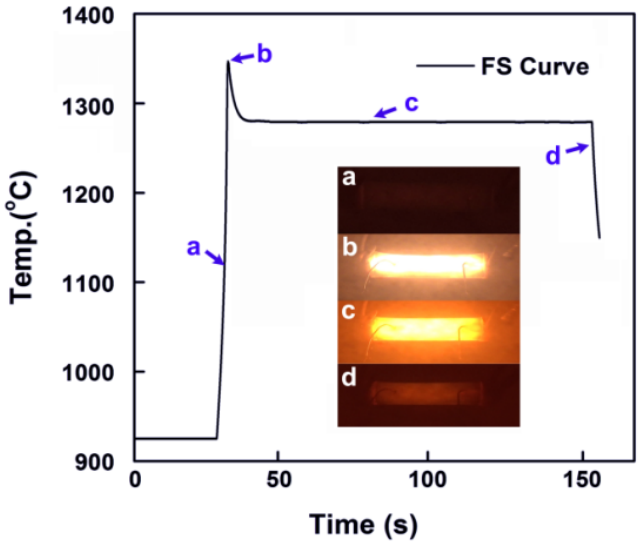

Figure 2. Temperature as a function of time in flash sintering with a soaking time of 2 min. Insert: video images at (a) 30s, (b) 32.5s, (c) 80s and (d) after power off.

Conventional Sintering:

For conventional sintering, the specimens were heated in a tube furnace in air from room temperature to the soaking temperatures of 1150 °C ~ 1500 °C at a heating rate of 5 °C /min. The soaking time was 1 hour for all the runs. The cooling rate was also 5 °C /min.

Fast Firing:

The fast firing experiments were also carried out in the tube furnace, with a steady state

temperature of 1315°C. The samples were attached to a long C-type thermocouple which was used both to insert the specimens into the ready-heated furnace and to record the specimen temperature. To obtain the highest heating rates possible, the samples were inserted rapidly to the hot zone of the furnace. After sintering for various times (30 s, 1 min, 2 min, 3 min, 5 min and 60 min), the samples were quickly withdrawn from the furnace and cooled in air. Details of the temperature profile obtained can be seen in [14].

SHS:.

The SHS reaction between Ni and Al was utilized as a thermal source to supply the 3YSZ compact with heat. The SHS reactants consisted of Ni (74 μm, 99.8%) and Al (29 μm, 98.7%) powders in a molar ratio of 1:1, with 18-30 mol. % diluents (TiC, 2 μm, 99.5%) added to adjust the temperature-time profiles of 3YSZ to reach peak temperatures of 1193-1540 °C. During all the SHS runs, it only took less than 10 s from room temperature to the peak and a maximum of ~1 minute to cool back to less than 1200 C. Details of the temperature profile for the 1301 °C specimen can be seen in [14].

Characterisation:

Sintered densities were measured by the Archimedes method. For the flash sintered specimens, only the section between the electrodes was measured. The grain sizes of sintered specimens were measured using at least 100 linear intercepts from single FESEM (JEOL 6500F) micrographs of polished and etched surfaces and using a multiplying factor of 1.56. Thermal etching was for one hour at 1100 °C, except for specimen sintering temperatures of less than 1200 °C, for which 100 °C below the specimen sintering temperature was used. More detailed observations were performed by a HRTEM (FEI Talos- F200s). The thin-foil samples for TEM examination were prepared from the sintered body in a focused ion beam instrument (FIB, Zeiss Auriga). The parameter changes during the flash sintering process were recorded by the controlling software. The linear shrinkage of FS samples during sintering was measured from the video images. This information was used to estimate $A(t)$ in eq. (1).

Table 1. Grain size and relative density in various sintering methods.

Sintering method	No.	Maximum sample temperature (°C)	Nominal heating rate (°C/s) [a]	Steady state sample temperature (°C)	Soaking time (s) [b]	Relative density (%)	Grain size (nm)
Conventional Sintering (CS)	1	1150	0.083	1150	3600	82.6	110
	2	1200	0.083	1200	3600	95.7	140
	3	1250	0.083	1250	3600	99.4	170
	4	1300	0.083	1300	3600	99.7	230
	5	1350	0.083	1350	3600	99.8	260
	6	1400	0.083	1400	3600	99.9	360
	7	1500	0.083	1500	3600	100.0	530
Fast Firing (FF)	1	1315	50	1315	30	83.2	110
	2	1315	50	1315	60	88.7	120
	3	1315	50	1315	120	96.1	130
	4	1315	50	1315	180	99.7	150
	5	1315	50	1315	300	99.9	170
	6	1315	50	1315	3600	100.0	250
Self-propagating High-temperature Synthesis (SHS)	1	1193	159	n/a	6.7	89.7	120
	2	1287	125	n/a	5.8	98.3	180
	3	1301	339	n/a	5.8	99.0	200
	4	1313	568	n/a	5.6	99.6	230
	5	1540	1250	n/a	4.6	100.0	530
Flash Sintering (FS)	1	1347	94	n/a	0	82.1	110
	2	1347	94	1280	10	98.8	120
	3	1347	94	1280	30	99.7	120
	4	1347	94	1280	120	100.0	120

[a] The heating rate of No.1 SHS, No.1 and No.2 CS specimens are from 950-1150 °C. All the others are from 950-1250 °C

[b] The soaking times for the SHS specimens are defined as the time spent within 25 °C of the maximum

3. Results and Discussion

3.1 Relative density - grain size relationship

The relative densities and grain sizes of 3YSZ specimens sintered by the different methods are listed in Table 1 along with the heating rates and other sintering parameters. The relationship between grain size and density is shown in Fig.3 and a selection of the microstructures for dense specimens (>99%) obtained by the different sintering methods is shown in Fig. 4.

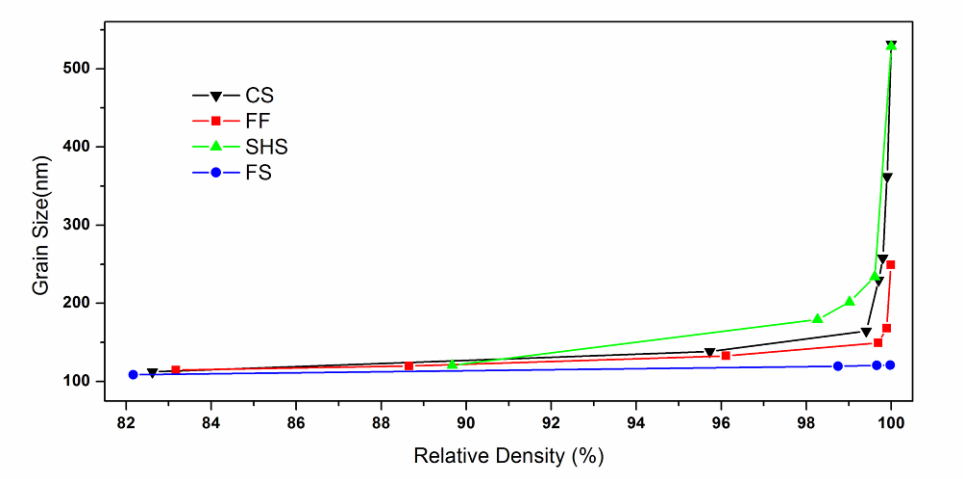

Figure 3. Grain size against relative density of specimens with various sintering methods.

For conventional sintering, the grain size-density relationship shows the classical form in which both relative density and grain size increase with temperature, with grain size increasing rapidly as full density is approached. Samples with a density of 99.4 % could be achieved by sintering for 60 min at 1250 ^{o}C, leading to a grain size of 170 nm. With higher sintering temperatures, the density increased further towards 100%, but this was accompanied by significant grain growth, finally reaching 530 nm at 1500 ^{o}C. There was no abnormal grain growth.

Vergnon et al [15] proposed the competition between grain growth and densification as a possible explanation for the improved sintering observed in fast firing. It is therefore of interest to compare the grain growth for the rapid heating methods with that for the conventional sintering results. The FF results show that a relative density of 99.7% could be achieved after only 3 minutes at 1315 ^{o}C (Table 1) and Fig. 3 shows that the grain growth was indeed lower for a given density than with conventional sintering. The FF grain size at 99.7% density was 150 nm, which is only 65% of that in the CS specimen at the same density.

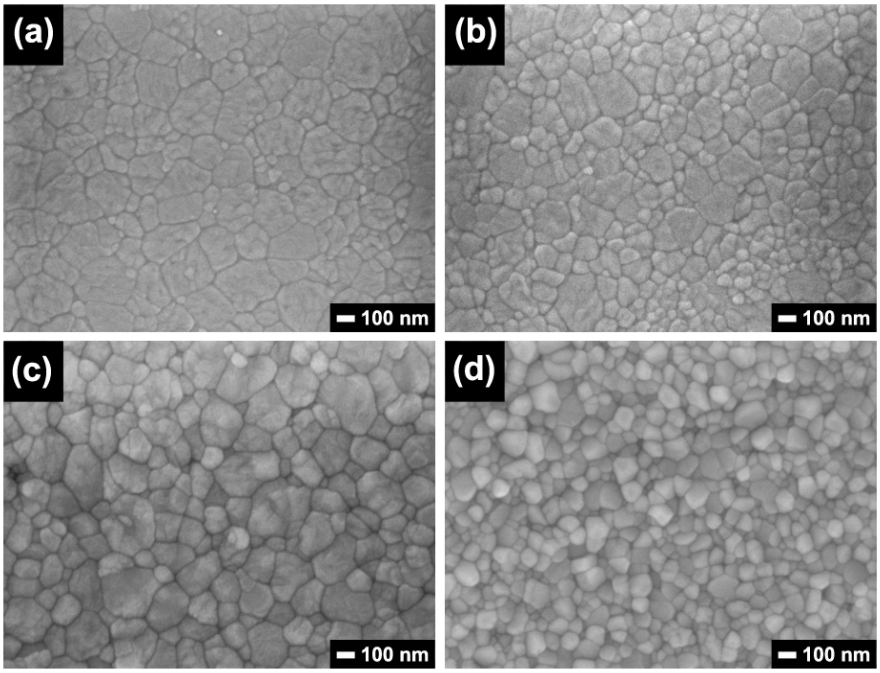

Figure 4. Morphology of fully dense samples with different sintering methods: (a) Conventional Sintering at 1350 ºC (heating rate 0.083 ºC/s, dwell time 3600s, relative density 99.8% and grain size 260 nm); (b) Fast Firing at 1300 ºC (heating rate 50 ºC/s, dwell time 180s, relative density 99.7% and grain size 150 nm); (c) SHS heating at 1301 ºC (heating rate 330 ºC/s, dwell time 6s, relative density 99.0% and grain size 200 nm) and (d) Flash Sintering at 950 ºC furnace temperature at a constant current of 0.5 A, reaching a maximum specimen temperature of 1347 ºC (heating rate 94 ºC/s, dwell time 30 s, relative density 99.7% and grain size 120 nm).

The FS specimens also follow this trend. A relative density of 99.7% could be achieved in only 30 s with a peak temperature of 1347 ºC and a steady state temperature of 1280 ºC (Table 1). In this case, the grain growth was very slight, even for the highest densities (Fig. 3), with a very uniform grain size of only 120 nm being retained to a relative density of 99.97%. Several mechanisms may contribute to this almost complete suppression of grain growth. The argument of Vergnon et al, that rapid heating enables the avoidance of a prolonged time at intermediate temperatures where grain growth may dominate, may be partly responsible.

As an additional mechanism, Ghosh et al. [19] have shown that the application of electric fields to YSZ can strongly inhibit grain growth, an effect attributed to the interaction of the field and the space charge at grain boundaries. This suppression of grain growth was shown to lead to

improvements in sintering [20]. The electric fields in the constant current part of the flash sintering cycle used here were about an order of magnitude higher than those used by Ghosh et al. so are easily sufficient to produce a significant inhibition of grain growth on the assumption that the effect does not show a maximum with field. Against that, Dong et al. [21] have also shown that the passage of high direct currents through YSZ at similar electric fields to those used here for significant lengths of time (20 hours in the most striking example) can lead to increased rates of grain growth owing to the consequent electrochemical reduction. It is presumed that the short flash sintering times used here did not allow sufficient electrochemical reduction for this effect to overcome the suppression of grain growth by the electric field-space charge interaction. For comparison, the total area-normalised charge passed in reference [21] was more than 4 orders of magnitude greater than in a typical flash sintering run in the present work.

An additional consideration is that the initial temperature peak of 1347 ^{o}C followed by a longer period at lower temperature (1280 ^{o}C) for the same FS specimen resembles "two step sintering" [22], in which grain growth becomes frozen at the lower temperature. This has previously been pointed out for the flash sintering of ZnO by Nie et al. [23]. It is clear from the CS results in Table 1, however, that significant grain growth can occur at temperatures below 1280 ^{o}C in the present case so the two-step effect does not apply. It is also noted that the FF and SHS specimens did not experience such a two step profile yet also sintered more rapidly than the CS specimen. The two-step effect is therefore not significant in explaining the rapid densification of 3YSZ.

Whilst there can be no doubt that the reduction in grain growth at a given density in rapid heating by FF and especially FS must contribute to the rapid sintering observed with these heating methods, the SHS results show that it cannot be the main explanation. This is because Fig. 3 shows that the SHS specimens had a larger grain size when approaching full density than specimens with the same density sintered using any of the other heating methods. Despite this, it was possible to sinter the SHS specimens to 99% dense in ~ 10 s. The reason for the difference in grain size between the FF and SHS results is not clear. It may be associated with a reducing atmosphere caused by the graphite foil used to separate the green compact from the SHS reactants. In this case, it is conceivable that the atmosphere also accelerated sintering. However, except for the very densest specimens, the SHS grain size exceeds those of the other methods by less than a

factor of 2 so it seems unlikely that the atmosphere can explain the acceleration in sintering rate of 1-2 orders of magnitude observed in Table 1 and reference [14]. In addition, Fig. 3 shows that the differences in grain size for any of the specimens only become apparent for relative densities of more than ~96%, and given that the acceleration in sintering is already apparent at lower densities (Table 1, Fig. 3), additional explanations must be sought.

3.2 Development of pore and neck geometry

In the last century, near consensus was reached that a major contribution to the success of fast firing comes from the avoidance of densification-free neck growth by surface diffusion. This is because surface diffusion is thought to have a lower activation energy than the diffusion mechanisms controlling densification, i.e. grain boundary diffusion and lattice diffusion, and therefore dominates at the low temperatures experienced for prolonged periods during slow, conventional heating. In contrast, fast firing avoids the detrimental effects of surface diffusion by heating the green body so quickly to the high temperature regime, where densification is dominant, that neck growth does not have time to occur as the specimen passes briefly through the damaging low temperature regime. [16,17,18].

The present ceramics have been examined for evidence of such history-dependent differences in microstructure. Figure 5 shows TEM micrographs comparing the microstructures of partially sintered CS and FS specimens. The appearance of the specimens is complicated by thin films of material redeposited in the pores during FIBing of the specimen. Nevertheless, it is evident that both specimens contain well developed necks and there is no clear difference in the pore *shape* on the scale of the necks sufficient to explain the great difference in sintering rates.

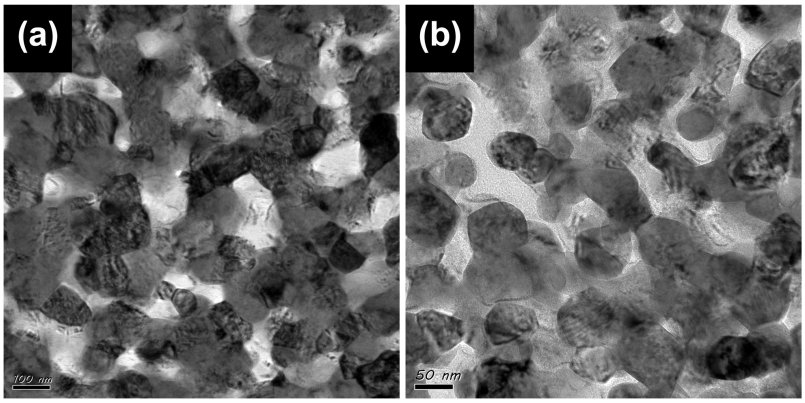

Figure 5. TEM micrographs of partially densified samples. (a) Conventionally sintered at 1150 ^{o}C with dwell time of 60 min, relative density 82.6% and (b) flash sintered at ~1300 ^{o}C without

soaking, relative density of 82.1%. Note the difference in magnification.

Clear differences in *size* of the pores and their coordination number are evident, however. Noting the difference in magnification, careful examination shows that the individual grains in Fig. 5 are of similar size in both specimens (see also Fig. 3). However, Fig. 5(a) shows that the solid sections between the pores in the CS specimens tend to consist of several grains, whereas the solid regions between the pores in the FS specimen in Fig. 5(b) are mainly single grains. This suggests that the pores are also larger in the CS specimen, and have a higher coordination number.

This contrast is seen more clearly in SEM micrographs of partially sintered specimens (Figs. 6, high magnification and 7, lower magnification). The CS specimen contained many pores which were significantly larger than the grain size, up to ~10 grain diameters (Figs. 6a, 7a), with correspondingly high coordination number, and the material in between the pores consisted of large groups of fully sintered grains. Such large pores would take a long time to remove by sintering.

These large pores were almost entirely absent in the FS specimen with similar density (Figs. 6d, 7d). Instead, the pores in the FS specimen were smaller than the grain size and were uniformly distributed, being observable at a majority of the triple points. Note that the small size of the pores combined with the effect of the thermal etching tends to obscure the porosity in the FS specimens but the presence of the porosity is clearly evident in the TEM micrograph of the same specimen in Fig. 5(b) as well as from the relative density (82.1%). Kim and Kim [24] have previously used mercury-intrusion porosimetry to show that fast firing with a heating rate of ~8 °C/s reduced the maximum pore size during sintering, and recent results by Kocjan et al. [25] have used the same technique to demonstrate reduced pore sizes in an initially mesoporous YSZ powder rapidly heated at ~4 °C/s.

The FF and SHS specimens (Figs. 6b, 6c, 7b and 7c) also had finer pore structures than those of the CS specimens, demonstrating that the electric field is not solely responsible for this difference. The porosity in the SHS specimens is not uniformly distributed, being greater in the interior of the specimen (Fig. 7b) than at the surface (Fig. 7c). The pores in the interior occur in clusters but the sizes of the individual pores within the clusters are small compared with the CS specimen. The pores at the surface, where the heating rate was highest, are particularly small and

of low coordination number. This is a consequence of the "outside in" heat flow causing the formation of a sintered shell on the rapidly heated outside of the specimen, which hinders subsequent shrinkage of the interior, resulting in turn in a higher porosity level. In larger specimens, Chen and Mayo found that this effect reduced the overall sintered density [26]. The rapid densification seen with the small specimens used here, despite some evidence of this restraining influence, confirms that rapid heating without an electric field is sufficient to cause ultra-fast densification and that a reduction in mean pore size is linked to this phenomenon.

The kinetics of sintering are highly sensitive to pore size. The densification rate for intermediate stage sintering, for example, is inversely proportional to the 3rd or 4th power of the microstructural scale, depending on the rate controlling diffusion mechanism [27], because larger pores reduce the driving force for densification and their greater separation for a given volume fraction of porosity increases the diffusion distance. The reduction in pore size of up to a factor of 10 therefore goes a long way towards explaining the rapid sintering rates of specimens with high heating rates.

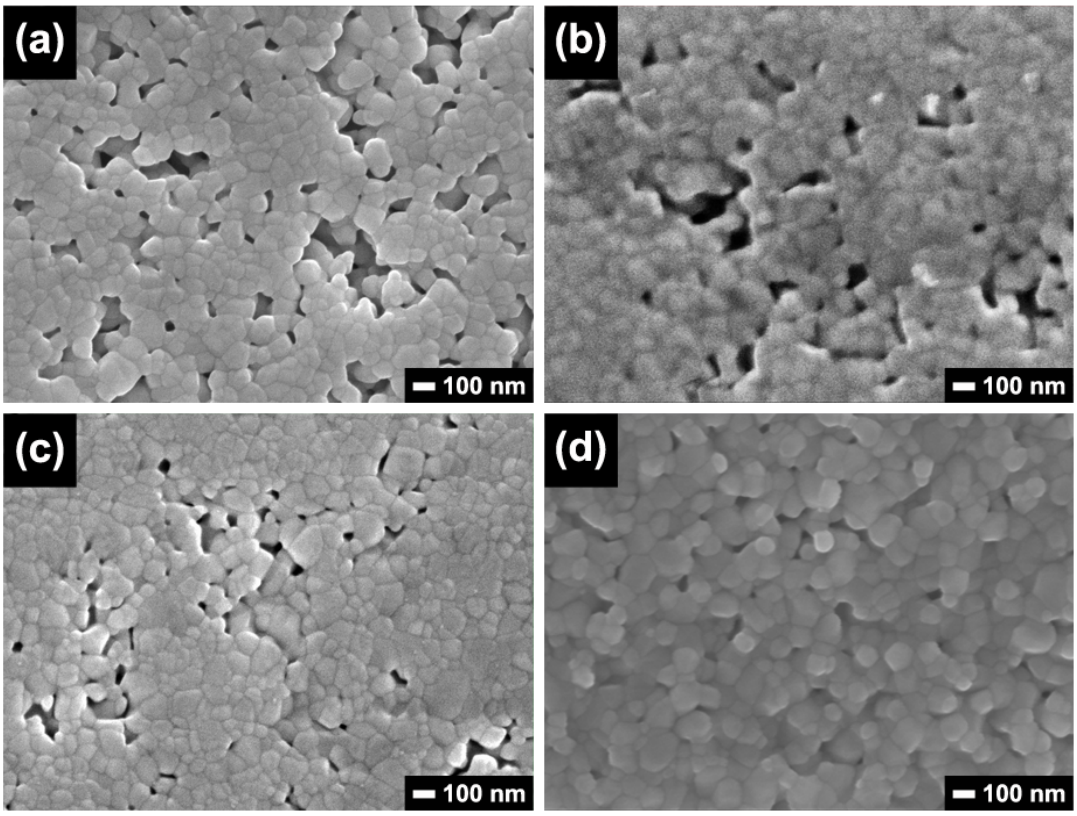

Figure 6. High magnification FESEM micrographs of partially dense samples with similar density and different sintering methods. (a) Conventional Sintering at 1150 ^{o}C for 60 min (relative density

82.6%); (b) Fast Firing at 1300 ºC for 1 min (relative density 88.7%); (c) SHS at 1193 ºC (relative density 89.7%) and (d) Flash Sintering with a maximum specimen temperature of 1347 ºC without soaking (relative density 82.1%).

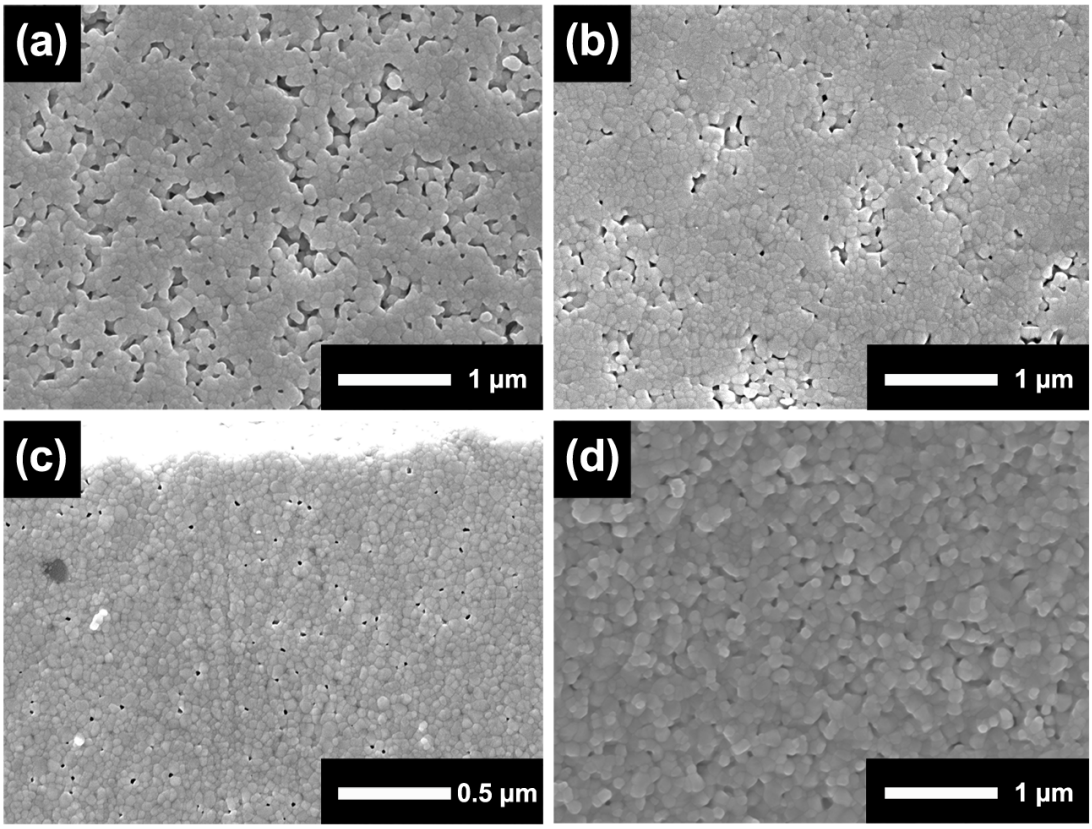

Figure 7. Lower magnification FESEM micrographs of partially dense samples with similar density and different sintering methods. (a) Conventional Sintering at 1150 ºC for 60 min (relative density 82.6%). (b) Interior section of SHS at 1193 ºC (relative density 89.7%). (c) Section showing near-surface region of the same SHS specimen as (b). (d) Flash Sintering with a maximum specimen temperature of 1347 ºC without soaking (relative density 82.1%).

This observation is a significant step forward in understanding the acceleration of densification observed in rapid heating of YSZ, with or without an electric field [14]. However, the origin of the difference in pore structure caused by rapid heating remains to be explained. An obvious possibility is a simple extension to the relevant length scale of the classical fast firing idea of competition between surface-diffusion controlled coarsening and densification. The pore network can coarsen to the scale greater than the grain size observed in the CS specimens by surface diffusion according to the Ostwald ripening driving force or the Rayleigh instability; rapid

heating would again avoid the low temperature regime where surface diffusion dominates. Other factors may contribute nonetheless, including the influence of grain boundaries with non-equilibrium composition or structure in rapid heating, as suggested in our previous work [14]. Ultimately, in order to understand ultra-fast firing, a better understanding of the development of large-scale pore structures in conventional sintering is also needed. This is often evident in conventional experimental results but is seldom discussed, possibly because most analytical models for sintering rely on idealised geometries having identical pores at all triple lines or grain corners of an array of identical grains.

3.3 Comparison of ultra-fast firing with and without an electric field

Like its companion paper [14], the present work shows that 3YSZ can be sintered in a few seconds without the use of an electric field by heating the powder compacts very rapidly. Similar conclusions have been reached for the case of ZnO by Zhang et al. [28]. The electric field is therefore not the primary cause of rapid densification in flash sintering. Very recently, Wang et al. [29] have also demonstrated rapid densification in other ceramics by external heating, though in contrast to the present work, in which the same maximum temperatures are used for all heating methods, Wang et al. use higher temperatures than for typical conventional sintering as an additional method of increasing the sintering rate.

There are, nevertheless, several advantages of using an applied electric field to provide the rapid heating necessary for ultra-rapid densification. Some of these are demonstrated in this work. The suppression of grain growth by the field (Fig. 3), for instance, undoubtedly acts as a secondary mechanism assisting sintering [19,20], and may also be a secondary contributor to the retention of a fine pore size (Figs. 6 and 7). The finer sintered grain size can also be expected to lead to superior mechanical properties.

There also appear to be effects of electric fields on sintering which are not simply a consequence of microstructural refinement. Careful experiments have recently shown an increase in sintering rates in yttria-doped ceria in the presence of moderate electric fields but in the absence of significant grain growth inhibition or change in pore structure [30,31]. However, the sintering rates in [30,31] were 2 to 3 orders of magnitude slower than those in the present work and it is emphasised that this field effect is also secondary to the ultra-fast firing effect described here.

A further advantage of using a contacting electric field to heat the specimens is that Joule heating allows relatively uniform heating throughout the interior of the specimen. The exterior heat sources used for ultra-fast firing without an electric field in this work were only successful here because of the very small dimensions of the powder compacts. This allowed heat to be conducted from the specimen surface to the interior in the short time-scale required. The use of similar methods on larger specimens of 3YSZ results in the formation of a dense outer shell early in the process which prevents the subsequent shrinkage of the interior, as described in Section 3.2 [26]. It is notable that the specimens in [29] also have at least one dimension which is small in scale, presumably for this reason. Flash sintering is therefore a good practical method of achieving ultra-fast firing for macroscopic components.

Conclusions

1. A strong history dependence of microstructure on heating rate has been observed in 3YSZ. The more rapid the heating rate, the finer the pore structure and the greater the coordination number for a given relative density, with or without the use of an electric field. In conventional sintering, for instance, many pores were up to 10 grain diameters in dimension and had correspondingly high coordination numbers whereas in flash sintered specimens, most pores were smaller than the grain size.

2. This difference in pore size is considered a major contributor to the significantly greater densification rate following rapid heating (again, with or without an electric field). The details of its origin remain to be determined but an extension of previous ideas concerning competition between surface diffusion and densification to a scale greater than the grain size offers one plausible explanation. Nonetheless, contributions from other effects such as non-equilibrium grain boundary compositions or structures remain a possibility.

3. Grain growth is suppressed more strongly in flash sintering of YSZ than in other rapid heating methods. This has previously been attributed to the interaction of the electric field with the space charge at the grain boundary [19].

4. Although an electric field is not necessary for ultra-fast densification, it has several benefits by way of secondary contributions to sintering, improved properties by microstructural modification and uniformity of heating compared with external heat sources.

Acknowledgement

The authors are grateful to the National Key Research and Development Plan of China (2017YF130310400), the National Natural Science Foundation of China (51902233，51521001, 51832003, and 51672197) and the Self-determined and Innovative Research Funds of WHUT (2019III059XZ).

References

[1] M. Biesuz, V.M. Sglavo. Flash sintering of ceramics. J Eur Ceram Soc 39 (2019) 115-143.

[2] M. Cologna, B. Rashkova, R. Raj, Flash sintering of nano grain zirconia in <5 s at 850 ◦C, J. Am. Ceram. Soc. 93 (2010) 3556–3559.

[3] Y.Y. Zhang, J.I. Jung, J. Luo, Thermal runaway, flash sintering and asymmetrical microstructural development of ZnO and ZnO-Bi_2O_3 under direct currents, Acta Mater. 94 (2015) 87–100.

[4] E. Bichaud, J.M. Chaix, C. Carry, M. Kleitz, M.C. Steil, Flash sintering incubation in Al_2O_3/TZP composites, J. Eur. Ceram. Soc. 35 (2015) 2587-2592.

[5] M. Cologna, J.S.C. Francis, R. Raj, Field assisted and flash sintering of alumina and its relationship to conductivity and MgO-doping, J. Eur. Ceram. Soc. 31(2011) 2827-2837.

[6] E. Zapata-Solvas, S. Bonilla, P.R. Wilshaw, R.I. Todd, Preliminary investigation of flash sintering of SiC, J. Eur. Ceram. Soc. 33 (2013) 2811–2816.

[7] V.M. Candelario, R. Moreno, R.I. Todd, A.L. Ortiz, Liquid-phase assisted flash sintering of SiC from powder mixtures prepared by aqueous colloidal processing, J. Eur. Ceram. Soc. 37 (2017) 485–498.

[8] R.I. Todd, E. Zapata-Solvas, R.S. Bonilla, T. Sneddon, P.R. Wilshaw, Electrical characteristics of flash sintering: thermal runaway of Joule heating. Journal of the European Ceramic Society, 2015. **35**(6): 1865-1877.

[9] I. J. Hewitt, A. A. Lacey and R. I. Todd. A Mathematical Model for Flash Sintering. Math. Model. Nat. Phenom., 10 6 (2015) 77-89 DOI: 10.1051/mmnp/201510607

[10] M Yoshida, S Falco, RI Todd, Measurement and modelling of electrical resistivity by four-terminal method during flash sintering of 3YSZ. Journal of the Ceramic Society of Japan 126 (2018) 579-590

[11] J. Janek and C. Korte, Electrochemical blackening of yttria-stabilized zirconia - morphological instability of the moving reaction front Solid State Ionics, 116, 181-195 (1999).

[12] M. Biesuz, V.M. Sglavo, Flash sintering of alumina: effect of different operating conditions on densification, J. Eur. Ceram. Soc. 36 (2016) 2535-2542.
[13] J.G.P. da Silva, H.A. Al-Qureshi, F. Keil, R. Janssen, A dynamic bifurcation criterion for thermal runaway during the flash sintering of ceramics, J. Eur. Ceram. Soc. 36 (2016) 1261-1267.
[14] W. Ji, B. Parker, S. Falco, J. Y. Zhang, Z. Y. Fu and R. I. Todd. Ultra-fast firing: Effect of heating rate on sintering of 3YSZ, with and without an electric field. J. Eur. Ceram. Soc., 2017, **37**(6): 2547-2551.
[15] P. Vergnon, F. Juillet, S.J. Teichner, Influence de la vitesse de montée en temperature sur le frottage d'alumine pure en particules homodispersée, Rev.Hautes Tempér. et Réfract. 3 (1966) 409-419.
[16] M.P. Harmer, E.W. Roberts, R.J. Brook, Rapid sintering of pure and doped Al2O3, Trans. Br. Ceram. Soc. 78 (1979) 22-25.
[17] M.P. Harmer, R.J. Brook, Fast firing: microstructural benefits, J. Brit. Ceram. Soc. 80 (1981) 147–148.
[18] D.L. Johnson, Ultra-rapid sintering of ceramics, in: D.P. Uskokovi´c, H. Palmour III, R.M. Spriggs (Eds.), Science of Sintering, Plenum Press, New York, 1989, pp.497-506.
[19] S. Ghosh, A. H. Chokshi, P. Lee, R. Raj, A Huge Effect of Weak dc Electrical Fields on Grain Growth in Zirconia. J. Am. Ceram. Soc. 2009, 92(8): 1856-1859.
[20] D. Yang, R. Raj, and H. Conrad, ''Enhanced sintering rate of zirconia (3Y-TZP) through the effect of a weak dc electric field on grain growth,'' J. Am. Ceram. Soc. 93 (2010) 2935–2937.
[21] Y Dong, H Wang, I-W. Chen., Electrical and hydrogen reduction enhances kinetics in doped zirconia and ceria: I. grain growth study, J Am Ceram Soc. 100 (2017) 876–886
[22] I-W. Chen, X. H. Wang, Sintering dense nanocrystalline ceramics without final-stage grain growth. Nature. 404 (2000) 168-171
[23] J Nie,Y Zhang, JM.Chan, S Jiang, R Huang, J Luo, Two-step flash sintering of ZnO: Fast densification with suppressed grain growth, Scripta Mater 141 (2017) 6-9
[24] D-H Kim and CH Kim, Effect of Heating Rate on Pore Shrinkage in Yttria-doped Zirconia, J Am Ceram Soc 76 (1993) 1877-8
[25] A Kocjan, M Logar and Z Shen, The agglomeration, coalescence and sliding of nanoparticles, leading to the rapid sintering of zirconia nanoceramics, Sci Reports 7 (2017) 2541
[26] D.J. Chen, M.J. Mayo, Rapid rate sintering of nanocrystalline ZrO2-3 mol%Y2O3, J. Am. Ceram. Soc. 79 (1996) 906-912.
[27] S-J. L. Kang, Sintering: Densification, Grain Growth, and Microstructure, Elsevier Butterworth-Heinemann, Oxford, 2005
[28] Y. Zhang, J. Nie, J. M. Chan and J. Luo, Probing the densification mechanisms during flash sintering of ZnO, Acta. Mater., 125, (2017) 465-475
[29] C Wang, W Ping, Q Bai, H Cui, R Hensleigh, R Wang et al., A general method to synthesize and sinter bulk ceramics in seconds, Science 368 (2020) 521–526

[30] C Cao, R Mücke, O Guillon, Effect of AC field on uniaxial viscosity and sintering stress of ceria, Acta Mater 182 (2020) 77-86

[31] C Cao, R Mücke , F Wakai, O Guillon, Viscous Poisson's ratio, bulk and shear viscosity during electrical field assisted sintering of polycrystalline ceria, Scripta Mater 178 (2020) 240-243